Mechanism of Co nanocluster burrowing on Cu(100)

J. Frantz and K. Nordlund
Accelerator Laboratory, P.O. Box 43, FIN-00014 University of Helsinki, Finland
(Received 21 August 2002; revised manuscript received 18 December 2002; published 26 February 2003)

Using a classical molecular dynamics method we have studied the burrowing mechanism of Co nanoclusters on a Cu substrate. We found that there are primarily two different mechanisms for the burrowing, depending on the configuration of the cluster after thermal deposition. Deposited clusters with an epitaxial configuration will burrow through vacancy migration along the Co-Cu interface, and nonaligned clusters burrow through disordered motion of atoms. The realignment of the nonaligned clusters was found to be due to a collective rotational movement of the whole cluster during the burrowing process. We discuss these results and perform a comparison with experimental and previously simulated results.

DOI: 10.1103/PhysRevB.67.075415 PACS number(s): 61.46.+w, 36.40.Jn, 36.40.Sx

I. INTRODUCTION

Recent experiments performed by Zimmerman *et al.* show that when a system consisting of Co nanoclusters which land thermally on a Cu substrate is heated up to 600 K the nanoclusters burrow into the substrate.[1] Transmission electron microscopy measurements performed on such samples showed that the fully burrowed nanoclusters are aligned with the substrate.

This phenomenon could prove to be crucial for the development of new high-density storage devices.[2] Supported magnetic nanoclusters on inert substrates, like noble metals, are considered to be good candidates because they satisfy both the requirements put on novel magnetic materials: size integration and highly localized magnetic moments.

Although the experiments establish the fact that this process exists and energy balance considerations[1] indicate that it is energetically favorable for the cluster to burrow, it is not clear what the mechanism of this process is.

The most important question on this matter concerns the burrowing mechanisms, what kind of mechanisms are involved and how they apply on different cluster configurations. The answer to this question could play a significant role in the optimization of the manufactoring process of nanostructured films of this nature.

How and when the nanocluster aligns up with the substrates lattice is certainly also an interesting question. For an alignment of crystals with different lattice constants to be possible, the lattice constants should not differ more than $\sim 3\%$.[3] This is certainly the case for Cu and Co where the difference is $\sim 2\%$.

Burrowing of Co nanoclusters on Cu has previously been examined by means of quasi–*ab initio* molecular dynamics (MD) simulations.[4,5] These works examine very small clusters, consisting of tens of Co atoms, which are burrowed into the Cu substrate. The main conclusions of these works are that the magnetic properties of the nanocluster would play a significant role in the burrowing process and that the cluster completely loses its initial shape. As we show in this paper, nanoclusters larger than ~ 1 nm in radius will show a different behavior due to the higher structural integrity.

This paper is organised as follows. In Sec. II we present the methods used for the simulations as well as the tools used for the analysis of the simulation results. Section III contains the results for our simulations, which is divided into four subsections depending on the type of observations: Sec. III A, landing; Sec. III B, epitaxially landed to nonaligned burrowing; Sec. III C, burrowing of nonaligned clusters; and Sec. III D, burrowing of epitaxial clusters. Section III E discusses other interaction models and considers results for the same simulations using alternative potential models. In Sec. IV we discuss the results and the implication of them, and in Sec. V we conclude the findings of this paper.

II. COMPUTATIONAL DETAILS

To investigate the burrowing we used classical molecular dynamics simulations.[6] The size of the substrates used ranged from 1000 to 140 000 atoms, and the size of the clusters was 500–6000 atoms. The systems used all had periodic boundary conditions in the directions of the surface plane and nonperiodic boundary conditions in the direction of the surface normal. The two bottom layers of the substrate were fixed, and the next three layers were softly cooled to ambient temperature. The time step length used was 3.91 fs and the trajectories of the atoms are calculated with the GEAR V algorithm.

The Co-Co interaction we used was described by the embedded-atom-method (EAM) interatomic potential of Pasianot and Savino[7] which is fitted to the elastic constants of Co and the vacancy formation energy. The Cu-Cu interaction was described with the EAM potential by Foiles[8] and the Co-Cu interaction was described with a potential constructed by Nordlund and Averback.[9] To rule out potential model-specific artifacts we also ran some simulations with two alternative potential models: the Cleri-Rosato model[10] and the model by Levanov *et al.*[11] The MD code employed in this work was PARCAS which has been used extensively in various scenarios; details of this code can be found in the literature.[9,12,13]

We emphasize that the empirical potentials are most reliable in predicting qualitative trends, since they cannot account for the electronic structure of the material and also have errors of the order of 10%–20% in the description of some of the quantities they are fitted to. Hence the numerical results given should be viewed with some caution. We do,

nevertheless, also give quantitive results to enable other scientists working in the field to check possible calculations done with other methods against our numbers.

The EAM models used[8,7,9] in the majority of the simulations can be motivated physically based on an effective-medium theory approximation of density functional theory.[14] For the elemental phases[8,7] the many-body potential formulation has been constructed such that it can describe all first-order elastic moduli of both Cu and Co correctly. It also gives a very good description of lattice vacancies, including migration properties, and a reasonable description of solid surfaces and melting.[15,14] In our previous work, we have found that the composite Co-Cu model also describes reasonably nonequilibrium phenomena at Co-Cu interfaces.[9] Since in the present work the most important physical characteristics of the materials can be expected to be the elastic properties, surface and interface energies, and the behavior of lattice vacancies, we believe the model used should be well suited for this study.

Two different types of initial configurations were used depending on what we wanted to simulate. The first configuration was an attempt to mimic the experimental conditions, and the second configuration was a recreation of a possible configuration of the nanocluster in some stage of its burrowing.

Initial configurations of the first type were created by creating a Co nanocluster in the shape of a Wulff polyhedron,[16] rotating it with a random angle and placing it above the substrate far enough to prevent interaction between it and the substrate. The Wulff polyhedron was used because experiments show that small Co clusters in equilibrium have the fcc rather than the hcp structure expected for bulk Co.[17] The shape of the nanocluster was determined by minimizing the surface energy of the Wulff polyhedron. After a short relaxation time at 300 K, the cluster was given a velocity corresponding to the thermal energy of 300 K in the direction of the substrate. After landing on the surface the system was relaxed for ~ 0.5 ns. After this the whole system was heated to 1000 K and simulated for 10–150 ns depending on whether anything interesting was observed. To determine the level of burrowing, snapshots of the system was taken with 0.5–1.0 ns intervals. These snapshots were visually checked, and to numerically analyze them, the atoms were quenched to 0 K and the number of Co atoms beneath the orginal surface was counted as well as the number of Cu atoms above the original surface.

Configurations of the second type were created by taking a perfect Cu lattice and replacing the Cu atoms in this lattice with Co atoms within a volume corresponding to an energetically correct Wulff polyhedron rotated by a certain angle or without rotation in an epitaxial configuration. These configurations were relaxed and run at different temperatures ranging from 600 to 1000 K at times of 0.5–10 ns. The simulation of these configurations was used to determine the burrowing mechanism and the processes behind the alignment of the cluster with the substrate. Simulations where the cluster was totally emerged into the substrate were also run, to test whether the cluster is able to reorient its lattice within the substrate bulk. In this last case, periodic boundaries were used in all directions.

Analysis of the nanocluster movement and alignment required the development of new analysis methods. A lattice analysis method was developed to analyze the alignment of the cluster compared to the substrate, and a grain analysis method was developed to identify the different grains of lattices inside the system. A dislocation analysis method based on a scheme introduced by Kelchner, Plimpton, and Hamilton[18] was further developed to be suited to our needs.

The lattice analysis method determines the lattice directions of atoms in the clusters compared to their nearest neighbors and compares these to the lattice directions of the substrate. The method calculates an index for each atom indicating its level of alignment. We call this index the epitax-factor F_{epi}. The grain analysis method determines the local environment of every atom and tries to identify the lattice unit vectors to its nearest neighbors. By then matching up all the lattice unit vectors, a map of the grains with the same lattice can be generated. Using this method boundaries between the cluster and the substrate can be identified. Both methods are described in more detail in Ref. 19.

The dislocation analysis method determines the neighborhood of every atom; in the analysis of this neighborhood it tries to identify six pairs of opposite neighbors relative to the considered atom. The vector for the considered atom to the atoms of every opposite pair is notated as $\mathbf{R}_i$ and $\mathbf{R}_{i+6}$, where i gives the pair index. As described in the original paper,[18] the centrosymmetry parameter is defined as follows:

$$P = \sum_{i=1,6} |\mathbf{R}_i + \mathbf{R}_{i+6}|^2. \tag{1}$$

The original description of this method has the disadvantage that the direction of the dislocation movement cannot be identified; this forces the analyst to guess about the type of dislocation depending on the values of P. To solve this inconvenience we introduce the centrosymmetric vector, which is defined as

$$\mathbf{P} = \left(\sum_{i=1,6} \mathbf{R}_i + \mathbf{R}_{i+6} \right) \Big/ 8; \tag{2}$$

this vector will show not only the direction of the dislocation movement but also show the size of the dislocation relative to the nearest neighborhood. The vector is divided by 8 to compensate for the number of contributing atoms and the distance of these atoms; this way the length of the vector will directly describe the distance the atoms moved to form the dislocation. This method is well suited for the analysis of edge and screw dislocations. These will order up the **P** vectors in planes or rows depending on the type of dislocation.

III. RESULTS

Several different cluster configurations were tested. We mainly focused on two different cluster sizes which were simulated extensively. The smaller cluster with a diameter of ~ 2 nm proved to undergo full contact epitaxy[20] on landing. This case proved to be quite uninteresting from the burrow-

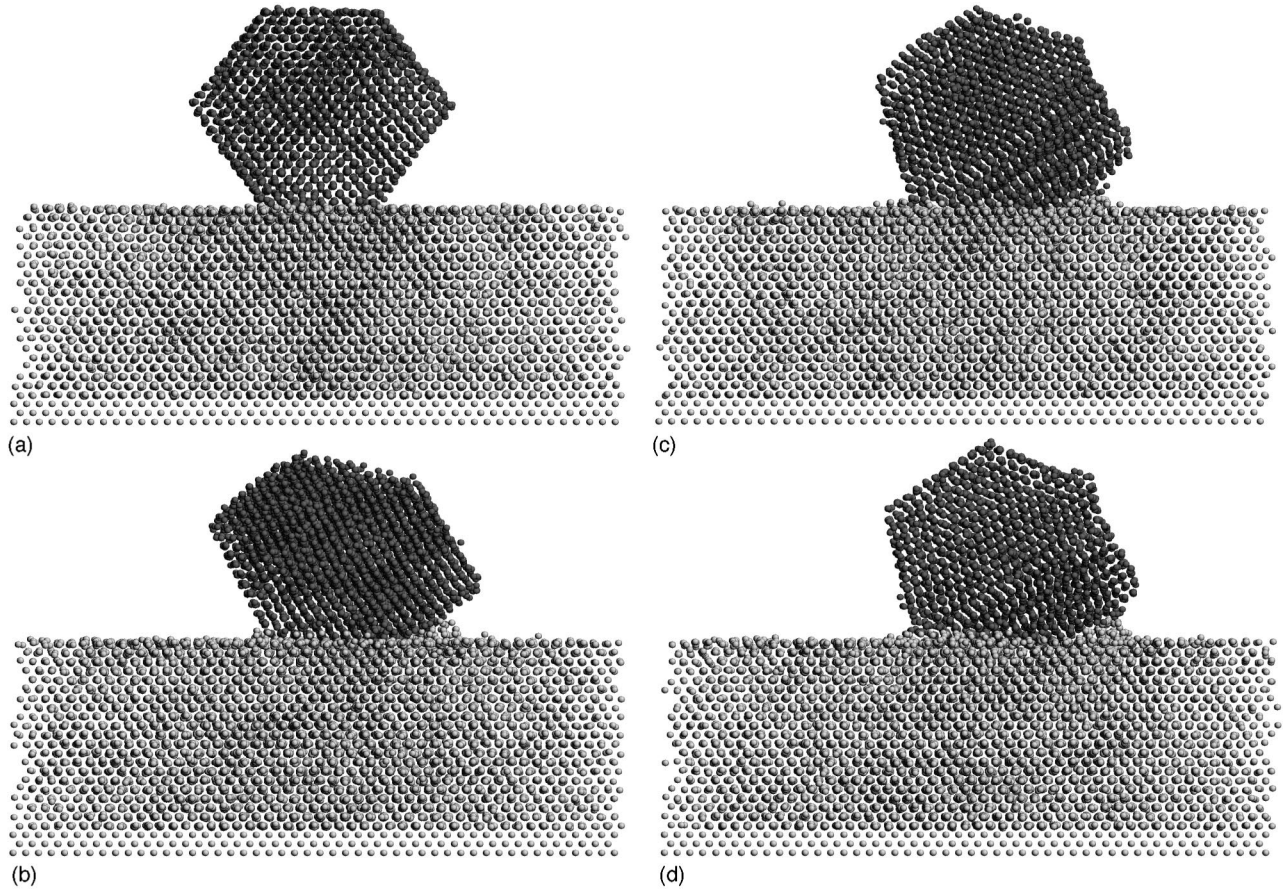

FIG. 1. Process of a cluster consisting of 4876 atoms lying on a ⟨100⟩ side on the substrate tilting over onto a corner. (a)–(d) correspond to the times 4 ps, 300 ps, 350 ps, and 10 ns. The darker spheres represent cobalt atoms, and the lighter spheres represent copper atoms. The figure is rotated so that the viewing direction is ⟨110⟩.

ing point of view; some small burrowing could be observed but mostly none at all. Previous work discussed in Sec. I (Refs. 4 and 5) describes such configurations.

The most interesting configurations were observed for the larger cluster which had a diameter of 5 nm containing 5477 atoms. In the next subsections we will refer to a cluster of this size. Figures 2, 3, and 4 all show results from the same simulation utilizing a cluster of this size.

A. Landing

We carried out 14 simulations where we allowed the clusters to land in different orientations and followed their behavior on the surface for 500 ps. These simulations showed that there are three different landed configurations for the cluster. The cluster can land on one of its ⟨100⟩ sides, which after some relaxation leads to a stable cluster on the substrate with matched lattices. The burrowing process in this case is very slow, but the cluster configuration can transform into a nonaligned one which starts burrowing. This is more closely examined in Sec. III B.

The second configuration is when the cluster lands on one of its ⟨111⟩ sides. This configuration is not stable, and the cluster will move around on the substrate at the simulated temperature of 1000 K. This configuration is the most inert considering burrowing, although the presence of the cluster on the surface leads to an increased amount of copper adatoms. If the temperature is dropped to 600 K, the cluster will find a local energy minimum configuration, where one of the ⟨110⟩ directions of the ⟨111⟩ plane matches one of the ⟨110⟩ directions of the substrate. This observation is already found in earlier work.[1]

If the cluster lands on a corner or an edge and forms a stable configuration in this state, the most interesting burrowing behavior can be observed upon the addition of thermal activation. The burrowing process in this case is more closely examined in Sec. III C.

B. Epitaxially landed to nonaligned burrowing

A cluster which has landed on a ⟨100⟩ side on the copper substrate may undergo a tilting process to reach a more reactive (from the burrowing point of view) nonaligned configuration. Figure 1 shows this tilting process of a cluster which has been landed on the substrate in an epitaxial configuration.

Figure 1(a) shows the configuration after 4 ps from the landing; at this stage in the simulation the landed cluster has relaxed and formed a epitaxial configuration with the substarte. The cluster spontaneously starts to tilt at about 100 ps,

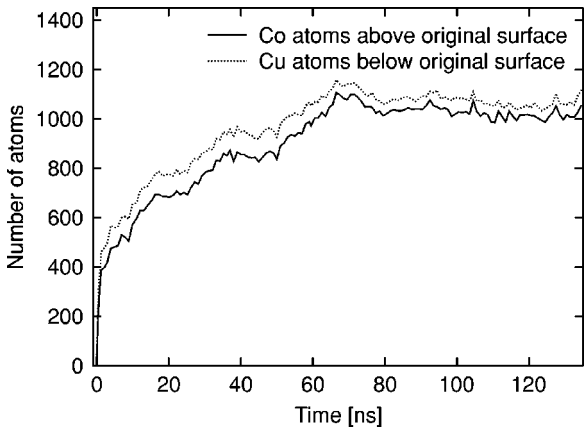

FIG. 2. Degree of burrowing for a cluster. Three different phases of the burrowing process can be observed in the figure: the first fast pulling phase lasts about 2 ns from the beginning of the simulation; then the slower rotational phase takes over, which lasts for about 70 ns until the $\langle 221 \rangle$ plane of the cluster matches up with the substrates $\langle 100 \rangle$ plane and the very slow vacancy migration burrowing phase starts.

and at 300 ps a observable tilting angle has been reached as shown in Fig. 1(b). As the simulation continues, the cluster tilts further as shown in Figs. 1(c) at 350 ps and 1(d) at 10 ns. As the cluster starts tilting its shape gets distorted but as it relaxes to its new local configuration it regains its original shape. One can also see that the cluster starts burrowing as it gains a nonaligned configuraton and that a considerable amount of Cu adatoms has surfaced during the process.

C. Burrowing of nonaligned clusters

The fastest burrowing can be observed with a configuration where a corner or an edge of the cluster forms the interface area with the substrate. The burrowing advancement originating from this nonaligned configuration is shown in Fig. 2. For these configurations the inclined planes of the cluster surfaces would be within the cutoff radius of the potential, which will be subject to strong attractive forces, leading to a rapid but short burrowing phase.

This rapid pulling phase of the cluster will last for a couple of nanoseconds and will stop when the inclined surfaces of the cluster have sunk into the substrate. This ''pulling'' burrowing effect requires that the cluster be large enough to maintain its structural integrity.[20] If the cluster is small (radius ~ 1 nm), the forces are strong enough to create a full contact epitaxy effect. In that case no nonaligned burrowing would be observed.

When the short rapid phase of the nonaligned burrowing is finished, a slower but longer-lasting process starts where the cluster slowly burrows by rotational movement. This process can be seen in Fig. 3. Previous work shows that dislocation motion can play a large role in the movement of clusters on substrates.[21] To identify the actual mechanism of the burrowing, we examined the system with the methods described in Sec. II. The movements of the atoms were individually examined throughout the simulations at 1 ns intervals; this examination showed traces of what could be interpreted as dislocations. However, an examination of the same snapshots at intervals as short as 50–150 ps with the dislocation analysis method showed no signs of dislocations activity. This fact was also confirmed by examinations with the grain analysis method which shows that the majority of the atoms in the Co cluster remain within the same local environment over ns time scales and no dislocations propagate through the cluster leading to the rotation. The same examinations showed no signs of atom slips in the substrate. Due to the fact that neither dislocations nor atom slip can explain the downward movement of the cluster, we conclude that the burrowing process is dependent on disordered movement of atoms along the Co-Cu interface.

Examining the movement of atoms in the system throughout the simulation, we noticed that the cluster is rotating as it is being burrowed. To examine the rotation of the cluster we used the grain analysis method to identify the lattice directions of the cluster. By comparing the lattice directions of the cluster at a given time we could then analyze how the cluster was rotating compared to the initial configuration. Comparison between the rotational speed and F_{epi} shows that the cluster is actually trying to reach an epitaxial configuration by rotation. This is shown in Fig. 4.

Closer analysis of the rotational movement of interval (B) in Fig. 4 in snapshots 50 ps apart showed that most of the rotation occurs during a time of 0.5 ns. Analysis of the movement of atoms in the cluster during this time showed that the cluster is moving at a roughly constant angular velocity in almost continous rotation. Analysis of the same snapshots with the dislocation analysis method showed that no dislocations are present during this rotation.

During the rotational movement of the cluster, the cluster will eventually find some matching planes with the substrate, even if the cluster is not completely aligned with the substrate. This matching is due to local energy minimum configurations of the Co-Cu interface. This can be seen in Fig. 2 as the last phase where no burrowing occurs on the simulated time scales. In the case depicted in this figure the $\langle 221 \rangle$ direction of the cluster aligns with the $\langle 100 \rangle$ direction of the substrate, forming a local energy minimum interface.

The simulations of clusters totally emerged in the bulk showed that if the lattice directions of the cluster differ more the 5° on all axes compared to the bulk, the cluster is not able to completely reorient its lattice directions to align up with the bulk lattice in 5 ns runs.

D. Burrowing of epitaxial clusters

If the cluster is not epitaxial after the landing, it will eventually reach an epitaxial configuration as it burrows due to the rotation of the cluster. When this configuration is reached, we observed that the burrowing slows down tremendously and the mechanism leading to the burrowing in the nonepitaxial phase no longer occurs. Examining atom movement in the system we came to the conclusion that the burrowing mechanism in this case is vacancy migration along the Co-Cu interface. Vacancies are created on the Cu surface which then move along the Co-Cu until it finally crosses the interface into the Co and move up on the Co side leading to a downward movement of Co atoms. This process can be seen in Fig. 5.

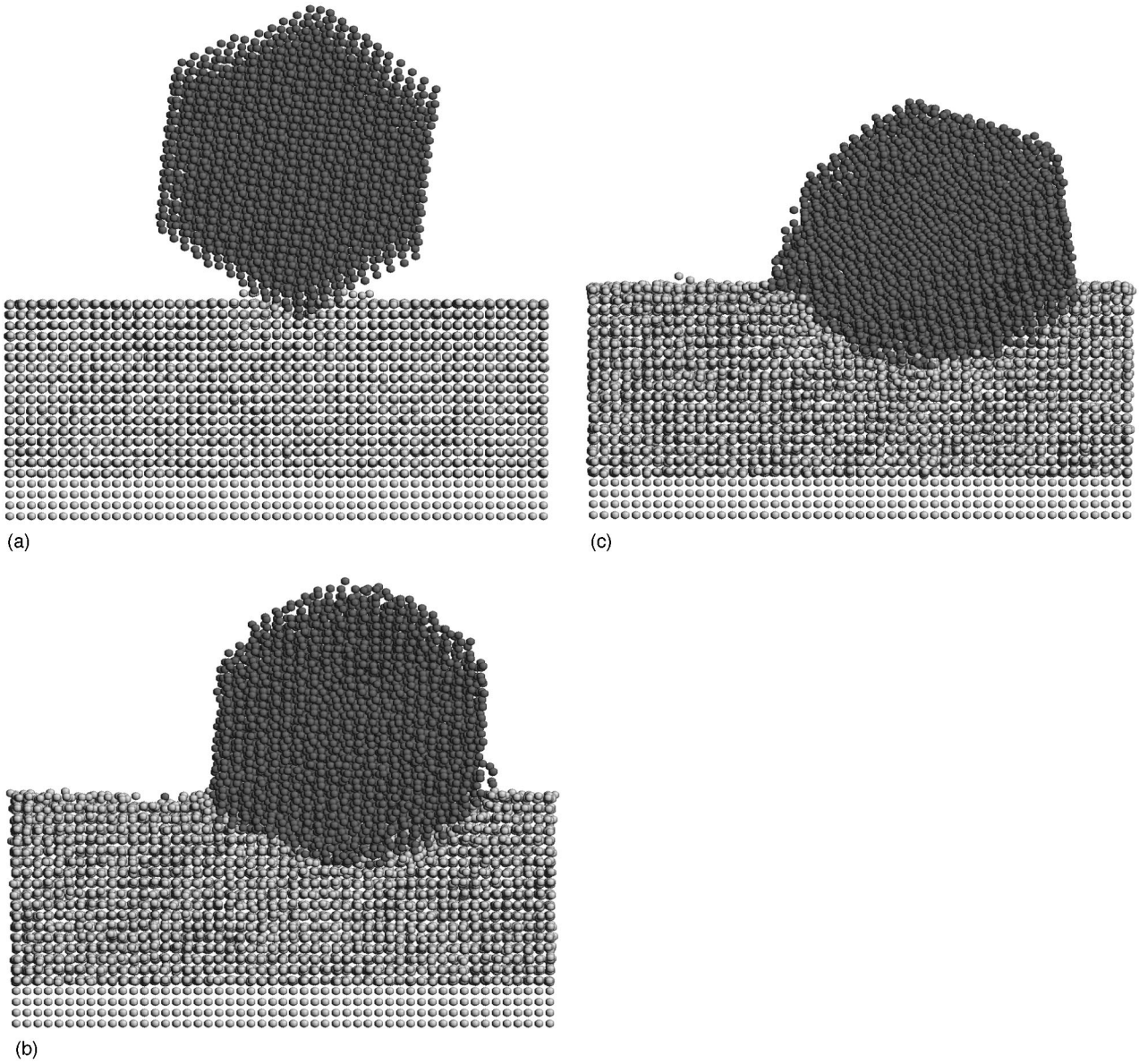

FIG. 3. How a cluster which has landed on a corner starts to burrow into the substrate. The figures are cross sections of a chosen part of the whole lattice to clarify the burrowing process. (a) shows the configuration when the cluster has relaxed on the surface, (b) shows how the cluster has burrowed after 20 ns, and (c) shows the situation at 60 ns.

Depending on the level of burrowing different numbers of vacancies movements can be seen in the system; when the cluster is burrowed one-quarter approximately two moving vacancies can be observed during a 5 ns simulation. If half of the cluster is burrowed, the number of moving vacancies is approximately 3, and in the case of three-quarters of burrowing, the number of vacany movements is approximately 4. Some of these vacancy migrations, but not all, can be seen to enter the Co side at some point and thus contribute to the downward movement of the Co atoms.

Offhand, it might seem unlikely that a high enough concentration of vacancies would be present to make the vacancy-mediated burrowing significant. However, one has to keep in mind that there is a large tensile stress at the Co-Cu interface region. For clusters in the size regime considered here, calculation of the atom-level virial shows that this stress can be of the order of -50 kbar. The relaxation volume of vacancies in Cu is about -3 Å^3 (Ref. 22), and hence the formation volume $+9$ Å^3. Thus the $P\Delta V$ term in the defect formation enthalpy is -0.28 eV, which is enough to raise the vacancy concentration by more then 2 orders of magnitude in Cu at 600 K (the experimentally used temperature) and to as high as 0.0001 at 1000 K. Considering that thousands of atoms are present in the interfacial region, the relatively large number of vacancies we observe in our 5 ns simulations is indeed quite reasonable.

From this vacancy concentration we have made a rough order-of-magnitude estimate of the burrowing time. For instance, for a nanocluster with 50 000 atoms, we estimate that there would be about 25 000 atoms in the strained interface

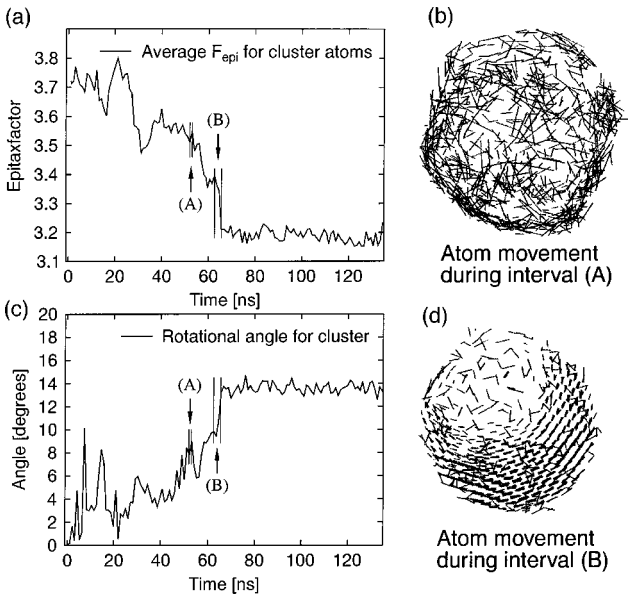

FIG. 4. The left-hand upper graph shows the F_{epi} and the lower figure shows the rotational angle for the cluster during the simulation. The rotational angle is calculated as the angle between the initial $\langle 001 \rangle$ direction of the cluster and current $\langle 001 \rangle$ direction at a given time. The figures on the right side show the movement of atoms during the intervals shown in the graphs. The bars in the right-hand side figures represent the movement of one atom during an interval of 1 ns. To avoid cluttering of the atom movement figures, only atom movements between 1.5 Å and 5 Å are shown. Note that the atom movement in (d) gets longer outwards from the center of the cluster; this is consistent with a rotation and not with a dislocation. Atom movements under 1.5 Å correspond to the thermal movement of the atoms and movements longer than 5 Å correspond to the surface migration of atoms. Interval (A) corresponds to a time of 1 ns, and interval (B) corresponds to a time of 3 ns.

region. We further estimate that each Co atom would have to move on average 100 times before burrowing is complete. To estimate the vacancy mobility we use the experimentally known migration rate of vacancies in Cu,[22] since most vacancies would be initially created in the Cu substrate. We arrive at a burrowing time of the order of 10 s at 600 K. In the experiments carried out at the same temperature, the burrowing was observed to be complete in minutes,[23] which is consistent with our rough estimate. Since experimental data on the time dependence of burrowing, or for temperatures below 600 K, are not available, there is not enough experimental data available to enable a more advanced comparison between the model and experiments..

The vacancy concentration can be expected to be further enhanced (in addition to the enhancement due to strain) right at the interface because vacancies tend to segregate at the interface to minimize the number of hetero-atomic bonds.[24] This could also decrease the burrowing time further from the estimate given above. Because the analysis method given in Ref. 24 is not directly compatible with our strain effect analysis, a deduction of the combined effect on the vacancy concentration is not straightforward and not attempted here.

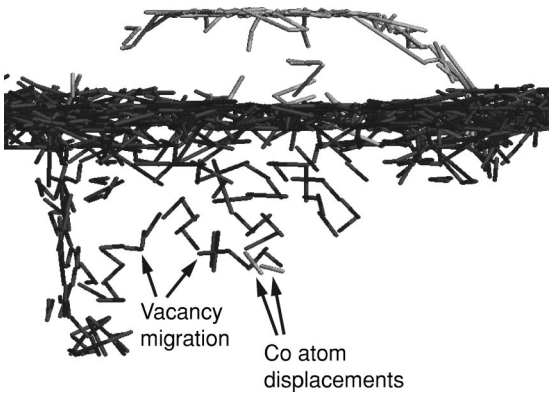

FIG. 5. Movement of atoms in a system consisting of an epitaxial 2 nm radius Co cluster three-quarters down in the substrate. The bars represent the movement of one atom during a time interval of 0.25 ns. The figure shows the atom movements during 1.25 ns. To avoid cluttering the whole figure, atom movements longer then 10 Å have been filtered away. Several chains (marked vacancy migration) which start on the surface and move along the Co-Cu interface can be seen. These represent vacancies created on the Cu side, which move along the surface, eventually passing through to the Co side. The net effect of this process is that Co atoms move downwards and thus the cluster burrows.

E. Other interaction models

In the simulations with the other potential models[10,11] we observed in 5 ns runs that 5 nm Co clusters burrowed into the Cu qualitatively quite similarly as the cluster described above. In the Cleri-Rosato model[10] we did not observe any discernible difference in the burrowing rate or mechanism. In the model of Levanov *et al.*[11] a significantly larger number of adatoms are created on the surface and the Cu also covers the Co cluster higher up than in the two other models. But also in this model the Co cluster burrowed in a similar manner, by disordered motion of atoms along the interface.

IV. DISCUSSION

The behavior of the Co clusters we observed in our simulations agrees very well with the experimental results, although our simulations have been done at 1000 K and the experiments were done at 600 K. This difference in temperature was adapted because the speed of the burrowing is strongly dependent on the temperature of the system and the molecular dynamics simulations have somewhat limited time scales. The experiments show that most clusters burrow but some do not.[23] According to our results this can be understood to be clusters which have landed with different configurations. The clusters which burrow are the ones landing on a surface with the same normal as the substrate surface or on a corner or an edge. The ones that do not burrow are the clusters landing on a surface with a differing normal compared to the substrate surface normal.

We did not observe any alignment of clusters totally immersed in the bulk in 5 ns runs, and indeed it is likely that because of the larger interface area, clusters deep in the bulk rotate slower than those only partially burrowed. Hence we

conclude that the clusters achieve the epitaxial configuration before they are fully submerged, through the rotation either at the surface or during the burrowing (see Sec. III C).

Burrowing of the epitaxial configuration could be simulated by means of kinetic Monte Carlo simulations if the lattice strain would be incorporated. However, this method could not be used for the nonaligned nanoclusters, because there are no available Monte Carlo methods for that kind of disordered configuration.

If the cluster lands on a $\langle 100 \rangle$ surface or when the cluster reaches an epitaxial configuration while burrowing, the mechanism for the continued burrowing is not disordered movement of atoms but vacancy motion over the Co-Cu interface. The difference in lattice constants will lead to an interface strain. This strain contributes to the creations of vacancies in the Cu substrate. The vacancies then move up towards the surface along the Co-Cu interface, leading to a Cu atom flow.

V. CONCLUSION

In this paper we have investigated the burrowing of Co nanoclusters on a Cu substrate using classical molecular dynamics simulations. Our results show that the mechanism of the burrowing is strongly dependent on the configuration of the cluster lattice compared to the substrate lattice. In the case of an epitaxial cluster on the substrate the mechanism is found to be vacancy migration along the Co-Cu interface. If the cluster initially is lying on an edge or a corner, the burrowing mechanism is disordered motion of atoms along the Co-Cu interface. The burrowing in this case is considerably faster than for the epitaxial case. In the case where the cluster has landed on a cluster surface with a normal different from the substrate surface normal, no burrowing was observed.

As for the mechanism of the alignment of the burrowed cluster, we found that this is due to the rotational movement of the cluster during nonepitaxial burrowing.

ACKNOWLEDGMENTS

The research was supported by the Academy of Finland under Project No. 73722 and by the University of Helsinki under the NAPROMA project. Grants of computer time from the Center for Scientific Computing in Espoo, Finland are gratefully acknowledged. We also want to thank Yinon Ashkenazy and Bob Averback for helpful discussions.

[1] C. Zimmermann, K. Nordlund, M. Yeadon, J. M. Gibson, R. S. Averback, U. Herr, and K. Samwer, Phys. Rev. B **64**, 085419 (2001).

[2] *Special Issue on Magnetoelectronics*, Phys. Today **84(4)**, 24–25 (1995).

[3] J. W. Mayer and S. S. Lau, *Electronic Materials Science For Integrated Circuits in Si and GaAs* (MacMillan, New York, 1990).

[4] J. Izguierdo, D. I. Bazhanov, A. Vega, V. S. Stepanyuk, and W. Hergert, Phys. Rev. B **63**, 140 413(R) (2001).

[5] V. S. Stepanyuk, D. V. Tsivline, D. I. Bazhanov, W. Hergert, and A. A. Katsnelson, Phys. Rev. B **63**, 235 406 (2001).

[6] M. P. Allen and D. J. Tildesley, *Computer Simulation of Liquids* (Oxford University Press, Oxford, England, 1989).

[7] R. Pasianot and E. J. Savino, Phys. Rev. B **45**, 12 704 (1992).

[8] S. M. Foiles, Phys. Rev. B **32**, 3409 (1985).

[9] K. Nordlund and R. S. Averback, Phys. Rev. B **59**, 20 (1999).

[10] F. Cleri and V. Rosato, Phys. Rev. B **48**, 22 (1993).

[11] N. Levanov, V. S. Stepanyuk, W. Hergert, D. I. Bazhanov, P. H. Dederichs, A. Katsnelson, and C. Massobrio, Phys. Rev. B **61**, 2230 (2000).

[12] K. Nordlund, M. Ghaly, R. S. Averback, M. Caturla, T. Diaz de la Rubia, and J. Tarus, Phys. Rev. B **57**, 7556 (1998).

[13] M. Ghaly, K. Nordlund, and R. S. Averback, Philos. Mag. A **79**, 795 (1999).

[14] M. S. Daw, S. M. Foiles, and M. I. Baskes, Mater. Sci. Rep. **9**, 251 (1993).

[15] S. M. Foiles and J. B. Adams, Phys. Rev. B **40**, 5909 (1989).

[16] J. E. Hearn and R. L. Johnston, J. Chem. Phys. **107**, 4674 (1997).

[17] O. Kitakami, H. Sato, Y. Shimada, F. Sato, and M. Tanaka, Phys. Rev. B **56**, 13 849 (1997).

[18] C. L. Kelchner, S. J. Plimpton, and J. C. Hamilton, Phys. Rev. B **58**, 11 085 (1998).

[19] K. Meinander, J. Frantz, K. Nordlund, and J. Keinonen, Thin Solid Films, 2003 (to be published).

[20] M. Yeadon, M. Ghaly, J. C. Yang, R. S. Averback, and J. M. Gibson, Appl. Phys. Lett. **73**, 3208 (1998).

[21] Y. Askenazy, R. S. Averback, and K. Albe, Phys. Rev. B **64**, 205 409 (2001).

[22] P. Ehrhart, in *Properties and Interactions of Atomic Defects in Metals and Alloys*, edited by H. Ullmaier, Landolt-Börnstein, New Series III, Vol. 25 (Springer, Berlin, 1991), Chap. 2, p. 88.

[23] C. Zimmermann, M. Yeadon, M. Ghaly, K. Nordlund, J. M. Gibson, R. S. Averback, U. Herr, and K. Samwer, Phys. Rev. Lett. **83**, 1163 (1999).

[24] J.-M. Roussel and P. Bellon, Phys. Rev. B **63**, 184114 (2001).